



CONSTRAINT EFFECTS IN FRACTURE TOUGHNESS TESTING OF IRRADIATED RPV STEELS IN THE CAMERA PLUS PROJECT

Hieronymus Hein¹, Marco Kaiser², Julia Kobiela³, Johannes May⁴

¹ Chief Advisor, Framatome GmbH, Germany (hieronymus.hein@framatome.com)

² Technical Head Hot Cells, Framatome GmbH, Erlangen, Germany

³ Engineer, Framatome GmbH, Erlangen, Germany

⁴ Senior Expert, Framatome GmbH, Erlangen, Germany

ABSTRACT

The impact of constraint effects on the fracture toughness in the ductile-brittle transition region was investigated by fracture mechanics tests for irradiated RPV steels in the CAMERA Plus project to quantify additional safety margins in RPV integrity assessment. Such constraint effects are geometry and loading rate effects with impact on fracture toughness. Crack tip constraint effects change the fracture toughness either to higher (loss of constraint) or lower (increase of constraint) values. To study this specific loss of constraint effect experimentally, fracture toughness tests were performed in accordance to ASTM E1921 to determine the reference temperature T_0 for two irradiated RPV steels with SE(B) specimens of different crack aspect ratios a_0/W in the range between 0.1 and 0.5. The test results have shown a significant constraint effect in terms of T_0 . The T_0 results revealed additional safety margins (up to some 10 K in T_0 for the materials tested) in RPV safety assessment considering loss of constraint effects for materials with significant irradiation embrittlement. Even for a crack aspect ratio a_0/W of about 0.25 a significant reduction of T_0 was observed. There is also evidence of significant scatter of lower crack aspect ratios a_0/W in terms of standard deviation for each specimen batch which is caused by manufacturing of short fatigue pre-cracks with a pre-crack starter length of a few tenths of a mm. Therefore, the application of the ASTM E1921 homogeneity check (screening procedure) yields to homogeneity for the nominal values of $a_0/W=0.5$ but not for $a_0/W=0.1$ (target value). This is apparently caused by superposition of the inherent material inhomogeneity in particular of welds and the scatter (standard deviation) in a_0/W ratios of the single specimens used for the tests with $a_0/W=0.1$. Even if the fluence was somewhat different for the standard specimens with $a_0/W=0.5$ compared to the fluence of the specimens with shallow cracks, the impact is of secondary importance since the gradient in increase of T_0 is reduced in the high fluence range of the materials tested. In contrast, the shielding effect of the specimen material in the irradiation capsule was identified as an important factor that requires an appropriate assessment regarding the correctness of the specimen fluences and its impact on the reliability of T_0 determination. It is assumed that the quantification of constraint effects in particular for irradiated materials contributes to get best estimate safety margins in RPV safety assessments for long term operation.

INTRODUCTION

The deterministic approach for the safety assessment procedure for reactor pressure vessels (RPV) is based on fracture mechanical calculations and the comparison of transient depending loading curves with the materials resistance in terms of fracture toughness. For the determination of the material's resistance two fundamental concepts exist: the indirect RT_{NDT} concept and the direct Master Curve concept based on fracture mechanics tests. In the preceding research programs CARISMA, Hein et al. (2010), CARINA, Hein et al. (2014), and CAMERA, Hein et al. (2022) the application of the Master Curve approach was confirmed successfully for various RPV materials in the brittle and brittle-ductile material region up to high fluences representative for long term operation of nuclear power plants. With respect to the RPV proof of

safety during plant operation, in particular at integrity assessments for Pressurized Thermal Shock (PTS) and at elaboration of p-T curves, further relevant issues have been studied in these research programs such as the validity of fracture toughness curve and Master Curve respectively in the irradiated state at higher test temperatures (ductile material region), the verification of the WPS (warm pre-stress) effect in the irradiated state for representative load paths and materials, as well as the impact of material inhomogeneities on the fracture toughness.

The follow-up program CAMERA Plus aims at investigating the impact of constraint effects on the fracture toughness in the ductile-brittle transition region to quantify additional safety margins in RPV integrity assessment. Constraint effects, which are geometry and loading rate effects, appear at the crack tip and change the fracture toughness either to higher (loss of constraint) or lower (increase of constraint) values. Loss of constraint is observed among others for shallow cracks with crack aspect ratios a_0/W being significantly lower than the nominal value of 0.5 resulting from the requirement that the initial crack size, a_0 , shall be 0.5 of the specimen width, W , as stated in the testing standard ASTM E1921. Within CAMERA Plus this specific loss of constraint effect was investigated by fracture toughness tests in accordance to ASTM E1921 to determine the reference temperature T_0 for two irradiated RPV steels with SE(B) specimens of different crack aspect ratios a_0/W in the range between 0.1 and 0.5.

MATERIALS

The two RPV steels, one base material and one weld material (see Table 1), were pre-irradiated in several large-capacity capsules in the test nuclear power plant Kahl (VAK) at temperatures between 280 °C and 290 °C in the frame of several dedicated irradiation programs in the 1980s, Hein et al. (2022).

The base material labelled P7 BM is a low Ni/P forging with elevated Cu content (0.12 % Cu, 0.97 % Ni, 0.015 % P) manufactured by Klöckner company. The specimens were taken from an untested WOL-100X specimen that was irradiated in the VAK reactor to a neutron fluence of $3.64 \cdot 10^{19} \text{ cm}^{-2}$ ($E > 1 \text{ MeV}$).

The weld material labelled P16 WM is a high Ni weld material (0.08 % Cu, 1.69 % Ni, 0.012 % P) and was manufactured by the company Uddcomb. The specimens were taken from an untested WOL-100X specimen, and the neutron fluence of the specimens used for testing was $4.56 \cdot 10^{19} \text{ cm}^{-2}$ ($E > 1 \text{ MeV}$).

Table 1: Materials of the CAMERA Plus test matrix

Material code	Type	Material	Cu [%]	Ni [%]	P [%]	Material features	Fluence ^{*)} [n/cm^2] ($E > 1 \text{ MeV}$)
P7	BM	22NiMoCr3-7 (manufactured by Klöckner)	0.12	0.97	0.015	low Cu / Ni / P	$3.64 \cdot 10^{19}$
P16	WM	S3NiMo3/OP 41 TT (manufactured by Uddcomb)	0.08	1.69	0.012	high Ni	$4.56 \cdot 10^{19}$

*) estimated neutron fluences referring to available source material

MANUFACTURING OF SPECIMENS

P7 BM

Twelve SE(B)10x10 specimens were manufactured in T-L (transverse) orientation from the untested WOL-100X specimen BA2 irradiated in the VAK reactor to an averaged neutron fluence of $3.64 \cdot 10^{19} \text{ cm}^{-2}$ ($E > 1 \text{ MeV}$). The specimen removal was done by means of two plates A (specimens BA2A2-BA2A7) and B (specimens BA2B2-BA2B7) cut off from the WOLX-100 specimen as shown in Figure 1.

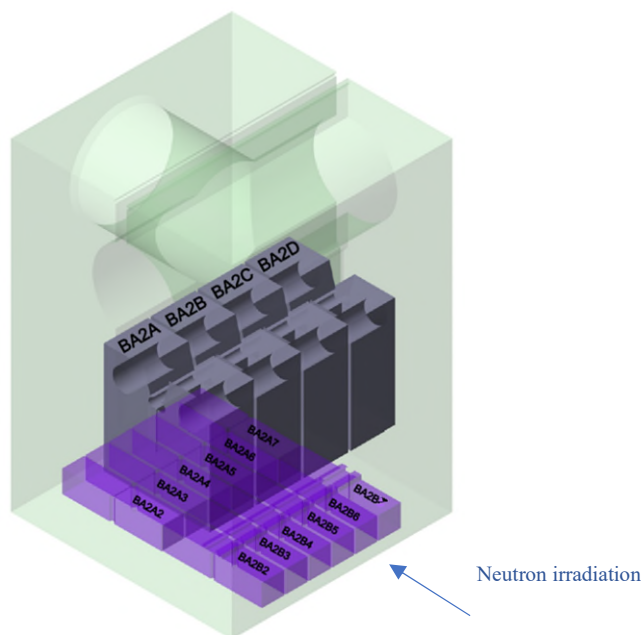


Figure 1. Removal of SE(B)10x10 specimens from WOL-100X specimen of material P7 BM

The six specimens of plate A were manufactured from SE(B)10x10 blanks where the existing 0.4 mm deep mechanical crack starter of the plate A specimens was extended to an initial target value of 1 mm for the crack length a_0 using a resonance machine to obtain a target relation between a_0 and specimen width W (a_0/W ratio) of 0.1. The six specimens of plate B were manufactured from SE(B)10x13 blanks ($W = 13 \text{ mm}$). This is because of the specific manufacturing process of the plate B specimens where the mechanical crack starter of 1 mm was extended to 3.5 mm by high-frequency vibration stress on a resonance testing machine followed by reducing the sample width W to 10 mm on both sides by means of electrical discharge machining (EDM) with a thin brass wire to obtain a target crack aspect ratio a_0/W of 0.1.

Two 45° side grooves of 0.5 mm radius were applied centrally into the specimen's sides, so that a test-ready SE(B)10x10 specimen with a net tests thickness B_N of 8 mm resulted. This manufacturing step as well as the obtaining of the required specimen dimensions was carried out by means of EDM with a thin brass wire. The manufacturing of the specimens was in accordance to ASTM E1921 with the exception of the used crack aspect ratio a_0/W of 0.1, which is nominally 0.5 resulting from the requirement that the initial crack size, a_0 , shall be $0.5W \pm 0.05$ as stated in the testing standard.

The final a_0/W -ratio of the six specimens each was 0.102 with standard deviation $\sigma = 15.2 \%$ (plate A), and 0.11 with $\sigma = 11.1 \%$ (plate B), respectively. The standard deviation σ is a criterion for the scatter in initial crack length a_0 and crack aspect ratio a_0/W of the specimen batch which is caused by the manufacturing process of the short fatigue crack.

Since plate B was in an irradiation position closer to the reactor core compared to plate A (shielding effect), the neutron fluence of the specimens taken from both plates was recalculated resulting in an average neutron fluence of $2.43 \cdot 10^{19} \text{ cm}^{-2}$ ($E > 1 \text{ MeV}$) for the specimens of plate A and $4.94 \cdot 10^{19} \text{ cm}^{-2}$ ($E > 1 \text{ MeV}$) for the specimens taken from plate B, respectively.

P16 WM

Twenty SE(B)10x10 specimens were manufactured in T-L (transverse) orientation from the untested WOLX-100 specimen GS9 irradiated in the VAK reactor to an averaged neutron fluence of $4.56 \cdot 10^{19} \text{ cm}^{-2}$ ($E > 1 \text{ MeV}$). The removal scheme for the SE(B)10x10 specimens is shown in Figure 2.

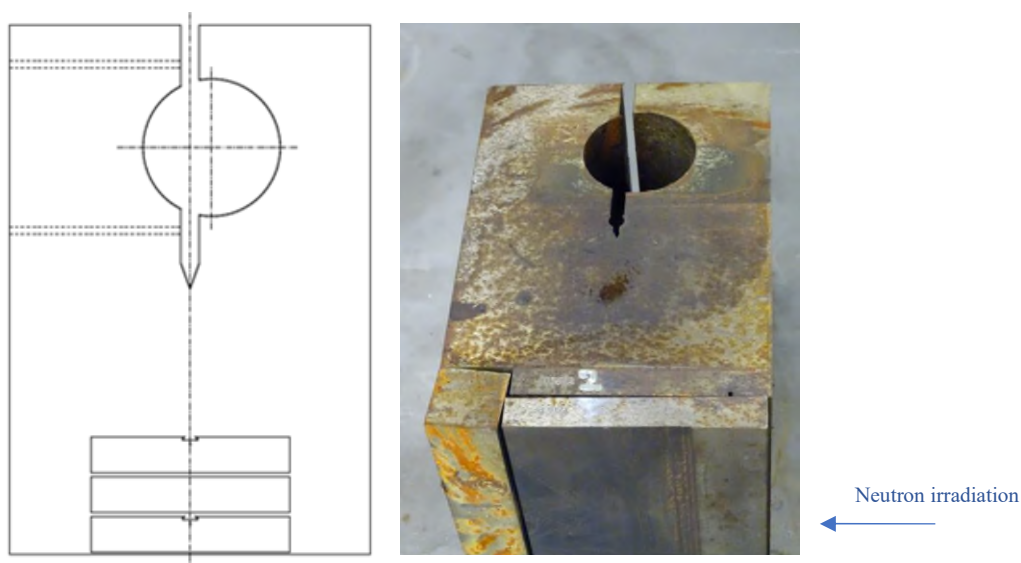


Figure 2. Removal of SE(B)10x10 specimens from WOL-100X specimen of material P16 WM

The specimen removal was done by means of three plates cut off from the WOLX-100 specimen as shown in Figure 2 (left). The extension of the weld in the plates was checked by etching to ensure that the SE(B) specimens consist of sufficient weld metal. The required specimen dimensions were obtained by EDM with a thin brass wire.

For seven SE(B)10x10 specimens, the mechanical crack starter of 1.5 mm length was manufactured first. Then, the existing 1.5 mm deep mechanical crack starter was extended to an a_0 target value of 2.5 mm using a resonance machine to obtain a target a_0/W -ratio of 0.25. The final a_0/W -ratio of these seven specimens was 0.254 with $\sigma = 13.6 \%$.

The remaining 13 SE(B)10x10 specimens were manufactured from SE(B)10x10 blanks where the existing 0.4 mm deep mechanical crack starter was extended to an initial target value of 1 mm for the crack length a_0 using a resonance machine to obtain a target a_0/W ratio of 0.1. The final a_0/W -ratio obtained was 0.137 with $\sigma = 19.8 \%$.

Two 45° side grooves of 0.5 mm radius were applied centrally into the specimen's sides, so that a test-ready SE(B)10x10 specimen with a net tests thickness B_N of 8 mm resulted. This manufacturing step and the obtaining of the required specimen dimensions was carried out by EDM. Again, the manufacture of the specimens was in accordance to ASTM E1921 with the exception of the used crack aspect ratios

a_0/W of 0.1 and 0.25, which are nominally 0.5 resulting from the requirement that the initial crack size, a_0 , shall be $0.5W \pm 0.05$ as stated in the testing standard.

Since the crack position of all SE(B) specimens concerned was in the same radial distance from the reactor core, the neutron fluence of those specimens is equally $4.56 \cdot 10^{19} \text{ cm}^{-2}$ ($E > 1 \text{ MeV}$).

DISCUSSION OF TEST RESULTS

The fracture toughness tests with the SE(B) specimens manufactured were performed in accordance to testing standard ASTM E1921. After testing of the specimens the progress of the fatigue crack fronts on the broken specimen halves were measured at nine defined positions according to standard ASTM E1921 in a contact free manner using digital photography and measurement technique. These measurement results were used as input for an evaluation program to calculate the stipulated values of the tested specimens in accordance with the standard. All test results are converted to a specimen width of $1T$ ($= 25.4 \text{ mm}$) according to ASTM E1921, to enable a specimen-width independent evaluation.

The calculation of the reference temperature T_0 at $100 \text{ MPa} \cdot \text{m}^{0.5}$ was carried out using the test temperatures and the fracture toughness $K_{Jc(1T)}$ values according to ASTM E1921. In compliance with the testing standard, the fracture toughness $K_{Jc(1T)}$ -test temperature (T)-diagram was generated using the corresponding limit curves and the $T_0 \pm 50 \text{ }^\circ\text{C}$ interval (Master Curve diagram). Finally, the screening criterion of ASTM E1921 was applied to assess whether the data set may not be representative of a macroscopically homogeneous material. In case of material inhomogeneity a simplified method was applied to perform a generally conservative estimate of the material's reference temperature T_{0IN} , that was used in lieu of T_0 , as described in the testing standard.

P7 BM

The Master Curve for the irradiated specimens of the P7 base material taken from plate A with $a_0/W = 0.102$ is shown in Figure 3, whereas the test results for the specimens taken from plate B are shown in Figure 4.

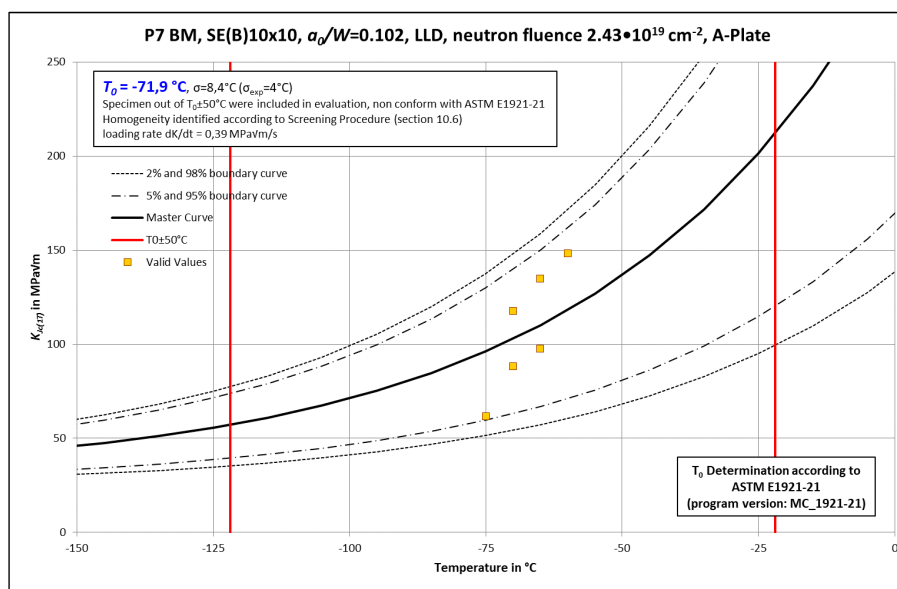


Figure 3. P7 BM, plate A - fracture toughness $K_{Jc(1T)}$ test temperature (T)-diagram, $a_0/W = 0.102$, LLD analysis, neutron fluence $2.43 \cdot 10^{19} \text{ cm}^{-2}$ ($E > 1 \text{ MeV}$)

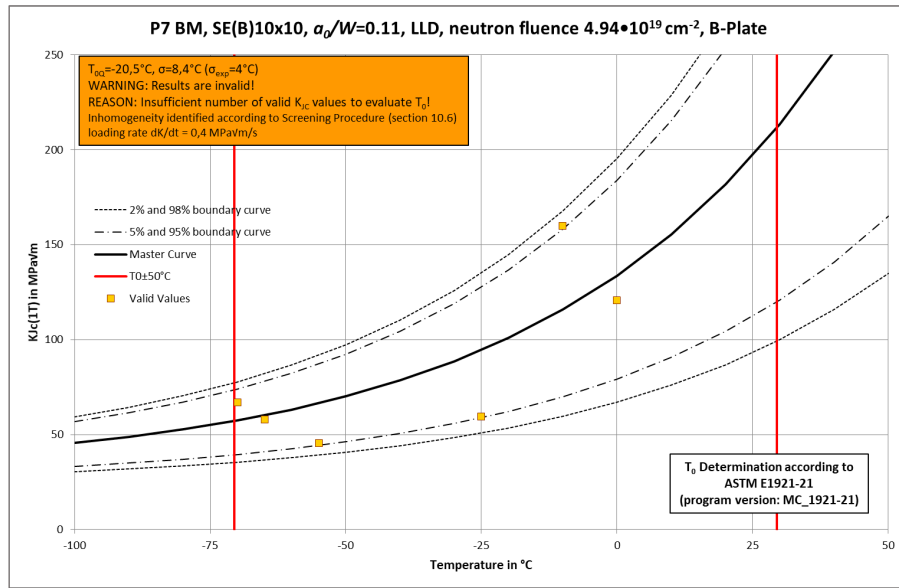


Figure 4. P7 BM, plate B - fracture toughness $K_{Jc(T)}$ test temperature (T)-diagram, $a_0/W = 0.11$, LLD analysis, neutron fluence $4.94 \cdot 10^{19} \text{ cm}^{-2}$ ($E > 1 \text{ MeV}$)

The determination of the reference temperature T_0 was based on load line displacement (LLD) diagrams recorded during the tests. The following reference temperatures T_0 and T_{0Q} (if invalid) in the transition range were calculated:

$$\begin{aligned} \text{P7 BM (plate A): } & T_0 = -71.9 \text{ }^\circ\text{C (LLD, } a_0/W = 0.102) \\ \text{P7 BM (plate B): } & T_{0Q} = -20.5 \text{ }^\circ\text{C (LLD, } a_0/W = 0.11) \end{aligned}$$

The application of the homogeneity screening procedure as described in testing standard ASTM E1921 reveals evidence for homogeneity of the tested specimen set plate A, and inhomogeneity of the tested specimen set plate B. The determination of T_0 for plate B based on crack mouth opening displacement (CMOD) analysis yields to a comparable $T_0 = -20.7 \text{ }^\circ\text{C}$, which is within the scatter band of testing. Hence, the difference is not significant. However, the results of the tested specimen set plate B are invalid because of insufficient number of valid values.

The test results of the P7 BM material obtained here for $a_0/W = 0.102$ (plate A) and $a_0/W = 0.11$ (plate B) were compared with already existing test results for $a_0/W = 0.50$ in terms of reference temperature T_0 based on the Master Curve, where the T_0 data for $a_0/W = 0.50$ were taken from the research program CARISMA, Hein et al. (2010). The comparison of all available T_0 results with different crack aspect ratios a_0/W is summarized in Table 2.

Obviously, a significant scatter of lower crack aspect ratios a_0/W in terms of standard deviation is observed for each specimen batch that is caused by the manufacturing process of the short fatigue cracks ($a_0/W = 0.102$ and 0.11 , respectively), whereas this is not the case for the nominal crack aspect ratio $a_0/W = 0.5$ with a longer fatigue length up to the final crack length used for testing. The application of the ASTM E1921 homogeneity check (screening procedure) yields to macroscopic homogeneity for $a_0/W = 0.5$ and 0.102 (plate A) but not for $a_0/W = 0.11$ (plate B) where inhomogeneity is indicated. This is apparently caused by superposition of the material inhomogeneity of the base metal and the scatter (standard deviation)

in a_0/W -ratios of the single specimens of plate B used for the tests. However, the plate B data set is invalid and therefore not considered for further assessment.

Table 2: Summary of T_0 test results for irradiated material P7 BM

Material and specimen type	Remark	Fluence ($E > 1$ MeV) [cm^{-2}]	a_0/W target	Average a_0/W measured	Standard deviation of a_0/W [%]	Analysis based on	T_0 [$^{\circ}\text{C}$]	T_{0IN} [$^{\circ}\text{C}$]
P7 BM SE(B)10x10	-	$4.45 \cdot 10^{19}$	0.5	0.50	0.9	CMOD	-22	-
	plate A	$2.43 \cdot 10^{19}$	0.1	0.102	15.2	LLD	-71.9	-
	plate B	$4.94 \cdot 10^{19}$	0.1	0.11	13.1	LLD	-20.5 ^{*)}	N/A
	plate B	$4.94 \cdot 10^{19}$	0.1	0.11	13.1	CMOD	-20.7 ^{*)}	N/A

^{*)} invalid

In order to be able to compare the T_0 results of the different aspect ratios (0.5 vs. 0.102) appropriately, the difference in neutron fluence ($4.45 \cdot 10^{19}$ vs. $2.43 \cdot 10^{19}$ cm^{-2}) has to be considered adequately. Taking into account the T_0 results for $a_0/W = 0.5$ from CARISMA, Hein et al. (2010) as shown by $RT_{T_0} = T_0 + 19.4$ K data in Figure 5, the T_0 value of the material P7 BM interpolated linearly to $2.43 \cdot 10^{19}$ cm^{-2} ($E > 1$ MeV) can be estimated to at least -50 $^{\circ}\text{C}$ ($RT_{T_0} \approx -30$ $^{\circ}\text{C}$). This estimation is a minimum because the linear increase of T_0 with increasing fluence is a conservative assumption since the reference temperature follows a power function with $A+B \cdot \Phi^n$ (with Φ as fluence) resulting in an even higher T_0 value. That means the T_0 of $a_0/W = 0.5$ at $2.43 \cdot 10^{19}$ cm^{-2} ($E > 1$ MeV) is higher than -50 $^{\circ}\text{C}$ and the minimum difference to the $T_0 = -71.9$ $^{\circ}\text{C}$ value of $a_0/W = 0.102$ is about 22 K showing a significant constraint effect in terms of lower T_0 .

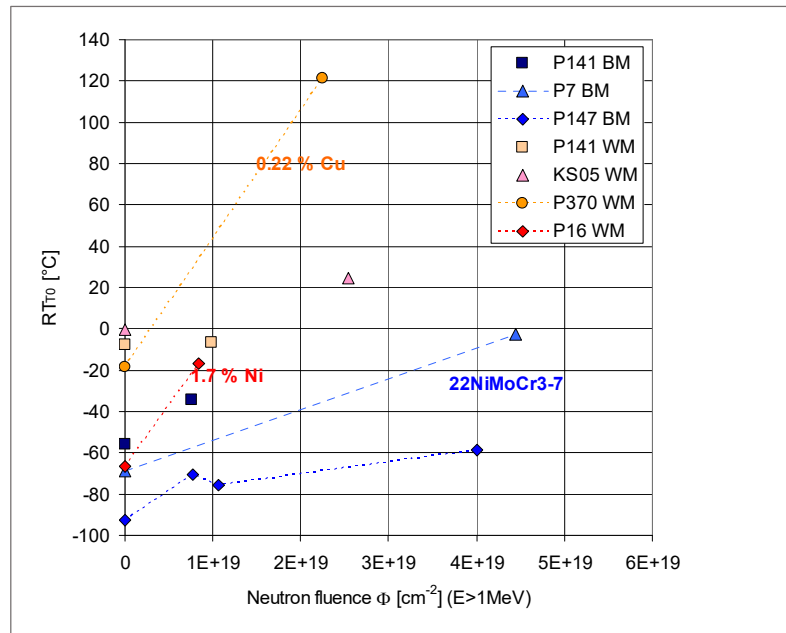


Figure 5. Reference temperatures RT_{T_0} of the CARISMA materials, Hein et al. (2010)

P16 WM

The Master Curves for the irradiated specimens of the P16 weld material with $a_0/W=0.254$ and $a_0/W=0.137$ are shown in Figure 6 and Figure 7, respectively.

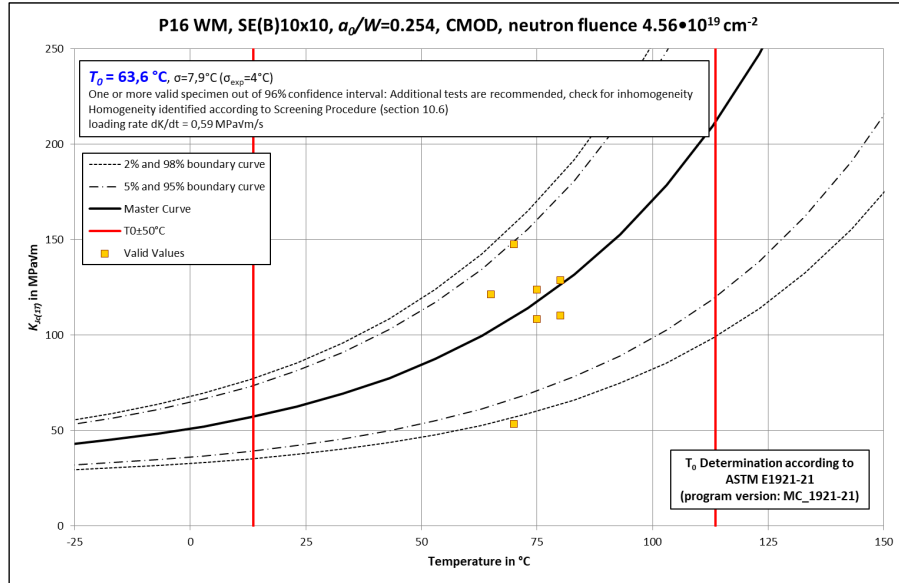


Figure 6. P16 WM - fracture toughness $K_{Jc(I,T)}$ test temperature (T)-diagram, $a_0/W = 0.254$, CMOD analysis, neutron fluence $4.56 \cdot 10^{19} \text{ cm}^{-2}$ ($E > 1 \text{ MeV}$)

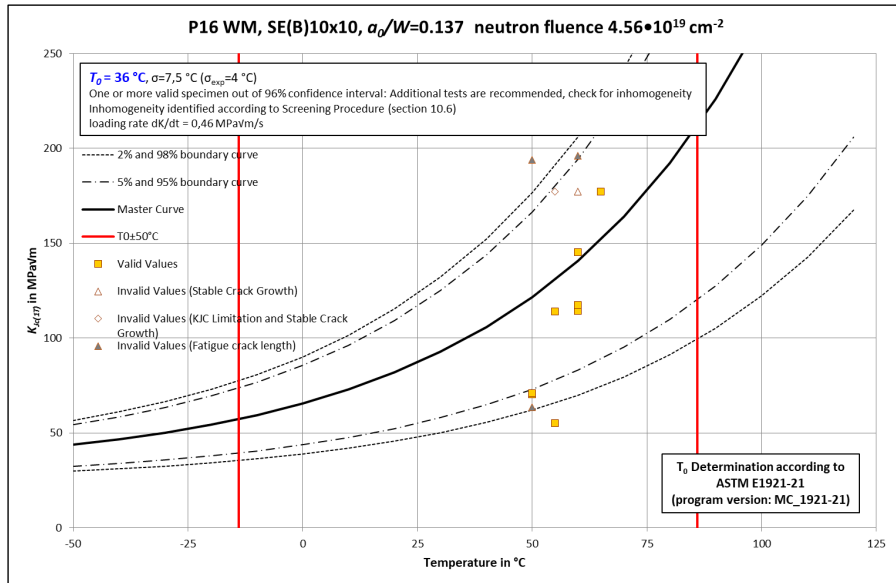


Figure 7. P16 WM - fracture toughness $K_{Jc(I,T)}$ test temperature (T)-diagram, $a_0/W = 0.137$, CMOD analysis, neutron fluence $4.56 \cdot 10^{19} \text{ cm}^{-2}$ ($E > 1 \text{ MeV}$)

The test results for the P16 WM material shown above can be compared with already existing test results for a crack aspect ratio $a_0/W = 0.51$ in terms of the reference temperature T_0 based on the Master Curve taken from the CARINA project, Hein et al. (2010).

The comparison of the T_0 results for all three crack aspect ratios is summarized in Table 3.

Table 3: Summary of T_0 test results for irradiated material P16 WM

Material and specimen type	Fluence ($E > 1$ MeV) [cm ⁻²]	a_0/W target	Averaged a_0/W measured	Standard deviation of a_0/W [%]	Analysis based on	T_0 [°C]	T_{0IN} [°C]
P16 WM SE(B)10x10	$5.43 \cdot 10^{19}$	0.5	0.51	2.2	CMOD	120.0	-
	$4.56 \cdot 10^{19}$	0.25	0.254	13.6	CMOD	63.6	-
	$4.56 \cdot 10^{19}$	0.25	0.254	13.6	LLD	66.6	
	$4.56 \cdot 10^{19}$	0.1	0.137	19.8	LLD	36.0	47.9

There is evidence of a significant scatter of the lower crack aspect ratios $a_0/W = 0.137$ and 0.254 , as indicated by the standard deviation for each specimen batch. Like for the P7 BM material this scatter for P16 WM material is caused by the manufacturing process of short fatigue cracks.

The application of the ASTM E1921 check for homogeneity (screening procedure) yields to homogeneity for $a_0/W = 0.51$ and 0.254 , respectively but not for $a_0/W = 0.137$. This is apparently caused by the superposition of the inherent material inhomogeneity of welds and the scatter (standard deviation) in a_0/W -ratios of the single specimens used for the tests with $a_0/W = 0.137$ where the conservative estimate of the reference temperature T_{0IN} according to the testing standard ASTM E1921 yields to a higher reference temperature if used in lieu of T_0 .

Nevertheless, looking to all test data shown in Table 3 a significant advantageous constraint effect in terms of T_0 is obvious in spite of the apparent superposition of material inhomogeneity and scatter in T_0 -ratios. The T_0 results reveal additional safety margins of some 10 K, even if based on T_{0IN} , with reference to the T_0 obtained for the nominal crack aspect ratio $a_0/W = 0.51$.

It should be noted that the fluence of $5.43 \cdot 10^{19}$ cm⁻² is somewhat higher for the standard specimens with $a_0/W = 0.51$ compared to the fluence of $4.56 \cdot 10^{19}$ cm⁻² of the specimens with the shallow cracks. However, the impact of the results is assessed as of secondary importance since the gradient in increase of T_0 is reduced in this high fluence range assuming a fluence dependence of T_0 described by the power equation $T_0 = A + B \cdot \Phi^n$.

CONCLUSIONS

The impact of constraint effects on fracture toughness was quantified by fracture toughness tests for two irradiated RPV materials with different crack ratios a_0/W resulting in different reference temperatures T_0 . The test results have shown a significant constraint effect in terms of T_0 and revealed additional safety margins of some 10 K in T_0 for the materials tested considering loss of constraint effects for materials with significant irradiation embrittlement. Even for a crack aspect ratio a_0/W of about 0.25 a significant reduction of T_0 was observed as exemplary shown for the highly irradiated high Ni weld P16 WM where the reference temperature T_0 was determined to 63.6 °C compared to 120 °C measured for $a_0/W=0.5$. There is also evidence of significant scatter of lower crack aspect ratios a_0/W in terms of standard deviation for each specimen batch which is caused by the manufacturing process of short fatigue pre-cracks with a pre-crack

starter length of a few tenths of a mm. Therefore, the application of the ASTM E1921 homogeneity check (screening procedure) for the materials tested yields to homogeneity for the nominal values of $a_0/W=0.5$ but not for welds with a lower crack aspect ratio of $a_0/W=0.1$. This is apparently caused by superposition of the inherent material inhomogeneity in particular of welds and the scatter (standard deviation) in a_0/W ratios of the single specimens used for the tests.

The impact of the fluence, which was somewhat different for standard and shallow crack specimens of the P16 WM material, is assessed of secondary importance since the gradient in increase of T_0 is reduced in this high fluence range. In contrast, the shielding effect of the specimen material in the irradiation capsule was identified as an important factor that requires an appropriate assessment regarding the correctness of the specimen fluences and its impact on the reliability of T_0 determination for a high fluence level.

It is concluded that the quantification of constraint effects in particular for irradiated materials may contribute to reveal additional inherent safety margins in RPV safety assessments for long term operation.

ACKNOWLEDGEMENT

The authors gratefully acknowledge the financial and technical support of support of the German Federal Ministry for the Environment, Nature Conservation, Nuclear Safety and Consumer Protection (sponsorship number 1501673), NPP Beznau/Axpo (Switzerland) and NPP Ringhals/Vattenfall (Sweden), and Framatome GmbH for the project CAMERA Plus.

REFERENCES

- ASTM E1921, Standard Test Method for Determination of Reference Temperature, T_0 , for Ferritic Steels in the Transition Range, Annual Book of ASTM Standards
- Hein, H., Keim, E., Schnabel, H., Seibert, T., Gundermann, A. (2010). "Final Results from the Crack Initiation and Arrest of Irradiated Steel Materials Project on Fracture Mechanical Assessments of Pre-Irradiated RPV Steels Used in German PWR," *Journal of ASTM International (2010)*, STP 1513 on *Effects of Radiation on Nuclear Materials and the Nuclear Fuel Cycle: 24th Volume*, <https://www.astm.org/jai101962.html>.
- Hein, H., Keim, E., Schnabel, H., Eiselt, Ch., Obermeier, F., Ganswind, J., Widera, M. (2014). "Final Results from the CARINA Project on Crack Initiation and Arrest of Irradiated German RPV Steels for Neutron Fluences in the Upper Bound," *Journal of ASTM International (2014)*, STP 1572 on *Effects of Radiation on Nuclear Materials: 26th Volume*, <https://www.astm.org/stp157220130113.html>.
- Hein, H., Kaiser, M., Lind-Tueysuez, V., May, J., Nicak, T., Obermeier, F. (2022). "Consideration of special effects for the application of an optimized fracture mechanics approach for the RPV safety assessment (CAMERA)," *Proc., 26th International Conference on Structural Mechanics in Reactor Technology*, SMiRT 26, 10 – 15 July 2022, Potsdam, Germany, <https://www.smirt26.com/Portals/smirt26/BB-Smirt26/Inhalt/th.2.h.2.pdf>.